

Influence of mixing the low-valent transition metal atoms ($Y, Y^* = \text{Cr, Mn, Fe}$) on the properties of the quaternary $\text{Co}_2[\text{Y}_{1-x}\text{Y}_x^*]\text{Z}$ ($\text{Z} = \text{Al, Ga, Si, Ge, Sn}$) Heusler compounds

K. Özdoğan* and B. Aktaş

Department of Physics, Gebze Institute of Technology, Gebze, 41400, Kocaeli, Turkey

I. Galanakis[†]

Department of Materials Science, School of Natural Sciences, University of Patras, GR-26504 Patra, Greece

E. Şaşıoğlu[‡]

*Institut für Festkörperforschung, Forschungszentrum Jülich, D-52425 Jülich, Germany
Fatih University, Physics Department, 34500, Büyükdere, İstanbul, Turkey*

(Dated: March 27, 2018)

We complement our study on the doping and disorder in Co_2MnZ compounds [I. Galanakis *et al.*, Appl. Phys. Lett. **89**, 042502 (2006) and K. Özdoğan *et al.*, Phys. Rev. B **74**, (2006)] to cover also the quaternary $\text{Co}_2[\text{Y}_{1-x}\text{Y}_x^*]\text{Z}$ compounds with the lower-valent transition metals Y, Y^* being Cr, Mn or Fe and the sp atom Z being one of Al, Ga, Si, Ge, Sn. This study gives a global overview of the magnetic and electronic properties of these compounds since we vary both Y and Z elements. Our results suggest that for realistic applications the most appropriate compounds are the ones belonging to the families $\text{Co}_2[\text{Mn}_{1-x}\text{Cr}_x]\text{Z}$ with $x > 0.5$ irrespectively of the nature of the sp atoms since they combine high values of majority DOS at the Fermi level due to the presence of Cr, and half-metallicity with large band-gaps. On the other hand the presence of Fe lowers considerably the majority density of states at the Fermi level and when combined with an element belonging to the Si-column, it even can destroy half-metallicity.

PACS numbers: 75.47.Np, 75.50.Cc, 75.30.Et

I. INTRODUCTION

Spintronics also known as magnetoelectronics is the newest growing branch of magnetism.¹ The main idea is to replace conventional electronics by a new kind of devices where the central role is played by the spin of the electrons and not the charge itself. This will allow the achievement of very low energy consumption in combination with other desirable features like the non-volatility for magnetic random-access memories (MRAMS), which have recently found application in automotive industry. The emergence and rapid growing of this research area brought in the center of scientific research the so-called half-metallic ferromagnets due to their possible applications.^{2,3,4,5,6,7} These materials are hybrids between metals and semiconductors or insulators, presenting metallic behavior for one spin-band and semiconducting for the other, and thus overall they are either ferro- or ferrimagnets with perfect spin-polarization at the Fermi level. de Groot and his collaborators in 1983 were the first to predict the existence of half-metallicity in the case of the intermetallic Heusler alloy NiMnSb .⁸ Several new half-metallic ferromagnetic materials and their properties have been initially predicted by theoretical ab-initio calculations and later verified by experiments.

Although the Heusler alloys like NiMnSb (known as half- or semi-Heusler compounds) have monopolized initially the interest, the last approximately five years the interest has been shifted to the so called full-Heusler compounds and mainly to the ones containing Co, like Co_2MnAl . These alloys date from 1971, when Webster

managed to synthesize the first Heusler alloys containing cobalt,⁹ and in early 90's it was argued in two papers by a Japanese group that they should be half-metals.¹⁰ These primary calculations paved the way and state-of-the-art first-principles calculations by Picozzi *et al.*¹¹ and Galanakis *et al.*¹² in 2002 confirmed the predictions of Ref. 10. Early experiments on these alloys were focused exclusively on the growth of the full-Heusler alloys,¹³ while latter experimental studies have also dealt the magnetic properties of the films,¹⁴ the role of defects and antisites,¹⁵ superlattices,¹⁶ transport properties¹⁷ and even the most complex subject of their incorporation in realistic devices.¹⁸

First principles calculations have been extensively employed to study the properties of the full-Heusler alloys. Several Heusler alloys have been shown to be half-metallic.^{12,19} Ab-initio calculations have shown that the surfaces²⁰ and interfaces of the full-Heusler compounds²¹ lose their half-metallicity but Hashemifar and collaborators have shown that it is possible to restore half-metallicity at some interfaces.²² Except interfaces states also temperature driven excitations^{23,24,25} and defects²⁶ seem to destroy half-metallicity. Also some other important aspect of these alloys like the orbital magnetism,²⁷ the structural stability²⁸ and the interplay of exchange interactions^{29,30} have been addressed in literature.

Over the last two years the interest in full-Heusler alloys containing cobalt has been focused on the so-called quaternary Heusler alloys, which are found to present half-metallicity as long as the corresponding perfect compounds are half-metals.³¹ The material of choice was

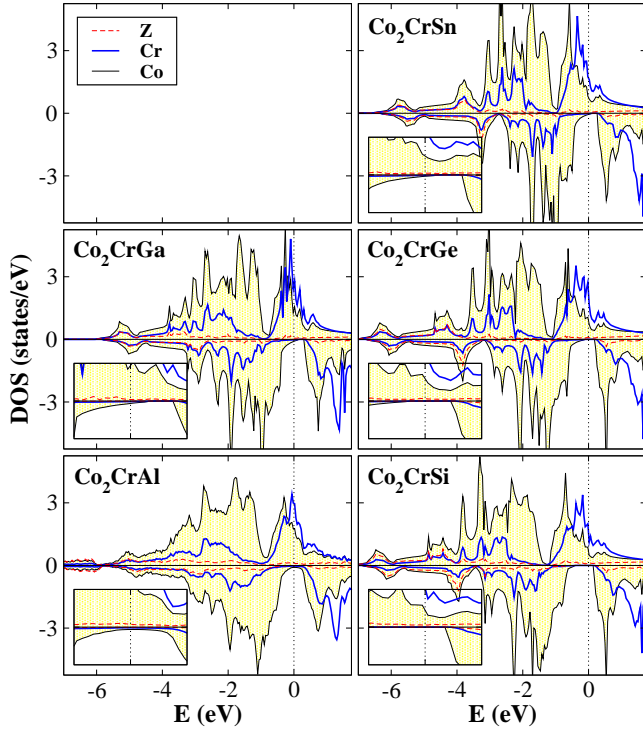


FIG. 1: (Color online) Atom-resolved density of states (DOS) for the Co_2CrZ compounds, where Z is Al, Ga, Si, Ge, and Sn. We have set the Fermi level as the zero of the Energy axis. In the onsets we have blown up the region around the Fermi level. Note that positive values of DOS refer to the majority-spin electrons and negative values to the minority-spin electrons.

$\text{Co}_2[\text{Cr}_{1-x}\text{Fe}_x]\text{Al}$. The half-metallicity has been predicted for all concentrations x ,³² and Miura et al have studied theoretically the stability of these compounds versus the creation of defects and antisites.³³ Also the family $\text{Co}_2[\text{Mn}_{1-x}\text{Fe}_x]\text{Si}$ has been extensively studied³⁴ due to the fact that ab-initio calculations, including the on-site Coulomb repulsion (the so-called Hubbard U), have shown that Co_2FeSi can reach a total spin magnetic moment of $6 \mu_B$ which is the largest known spin moment for a half-metal.^{35,36} Several experiments have been devoted to the study of the structural and magnetic properties of these quaternary Heusler alloys³⁷ and such films have been incorporated both in magnetic tunnel junctions³⁸ and spin-valves.³⁹

II. DESCRIPTION OF PRESENT CALCULATIONS

In a recent paper,⁴⁰ we employed the full-potential nonorthogonal local-orbital minimum-basis band structure scheme (FPLO)⁴¹ to study the effect of doping and disorder on the magnetic properties of the Co_2MnSi , Co_2MnGe , Co_2MnSn full-Heusler alloys. Doping simulated by the substitution of Cr and Fe for Mn in these

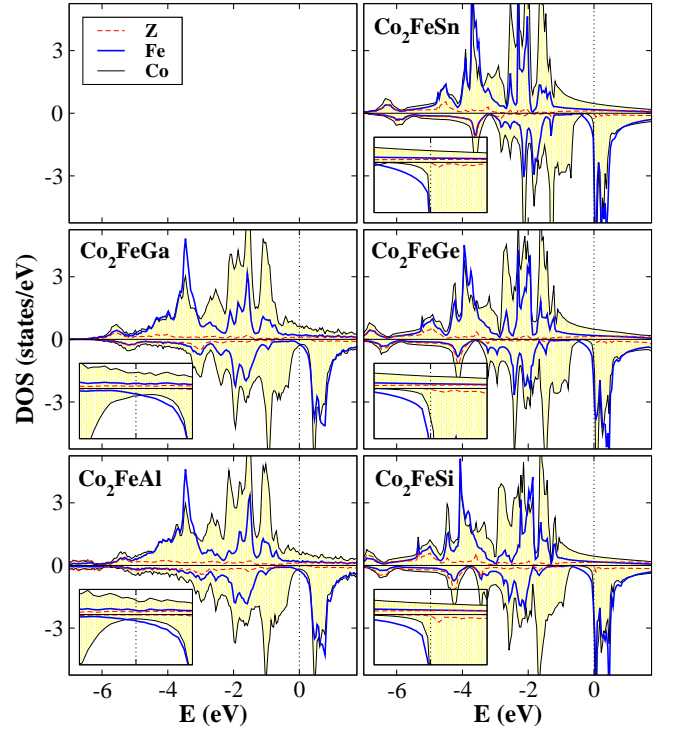


FIG. 2: (Color online) Same as Fig. 1 for the Co_2FeZ compounds where Z is Al, Ga, Si, Ge, and Sn.

alloys overall kept the half-metallicity. The effect of doping depended clearly on the position of the Fermi level, having the largest one in the case of Co_2MnSi where the Fermi level is near the edge of the minority-spin gap. Latter we expanded this work to cover also the case of Co_2MnAl and Co_2MnGa compounds⁴² which have one valence electron less than the previous ones. Also in that case a high degree of spin-polarization at the Fermi level was overall preserved. Finally for all five compounds we found that the creation of antisites severely affects the half-metallic character of the compounds.

In this manuscript we expand these two studies to cover not only the case of doping but all the families of resulting quaternary Heusler alloys; $\text{Co}_2[\text{Mn}_{1-x}\text{Cr}_x]\text{Z}$ and $\text{Co}_2[\text{Mn}_{1-x}\text{Fe}_x]\text{Z}$, with Z being Al, Ga, Si, Ge, Sn. For reasons of completeness we have decided to calculate also the case when we mix Cr and Fe atoms at the site occupied by the lower-valent transition metal atoms; $\text{Co}_2[\text{Cr}_{1-x}\text{Fe}_x]\text{Z}$ families. Since we change both the transition-metal atoms and the sp atoms, we get a global feeling of the behavior of the magnetic and electronic properties of these compounds. We have employed the FPLO electronic structure method as already stated in conjunction with the local-spin-density approximation (LSDA). The coherent potential approximation (CPA) was used to simulate the disorder. We have used the experimental lattice constants for the perfect compounds containing Mn^{43,44} and we have kept them constant when substituting with Fe or Cr since no evidence is known on

the exact behavior of the quaternary compounds. This tactic is different than the one used in Ref. 31 where it was assumed that the lattice constant varies linearly with the concentration. For the cases under study both methods give lattice constants within less than 1% difference and thus practically identical results. Finally we should note that we discuss half-metallicity in terms of total spin-moments since perfect half-metals show the Slater-Pauling (SP) behavior; the total spin moment in the unit cell is the average number of valence electrons minus 24.¹² Spin-polarization at the Fermi level is not considered since it remains very close to the perfect 100% and its exact value depends on computational details contrary to the total spin moments which were found to be more robust.

Before presenting our results we have drawn in Figs. 1 and 2 the atom-resolved DOS for the Co_2CrZ and Co_2FeZ compounds. On the left column of each figure are the cases with Z a *sp* element belonging to the IIIB column of the periodic table (Al and Ga) and in the right column the cases of IVB elements (Si, Ge and Sn). For the Co_2CrZ alloys the extra electron in the latter case occupies majority states leading to an increase of the exchange splitting between the occupied majority and the unoccupied minority states and thus to larger gap-width for the Si-, Ge- and Sn-based compounds with respect to the Al- and Ga-based alloys; a similar behavior was present also for the Co_2MnZ compounds.⁴² In the case of the compounds containing Fe the extra electrons with respect to Cr and Mn compounds lead to an overlap of the Co bonding and antibonding minority d-hybrids and the gap is already destroyed for the Co atoms. Moreover the unoccupied Fe states move lower in energy since the majority occupied Fe states are very deep in energy. The Al and Ga compounds keep a high degree of spin-polarization but the phenomenon is very intense for the Si, Ge and Sn compounds, which have 30 electrons per unit cell, and half-metallicity is destroyed. As argued by Kandpal et al, in the latter case (contrary to the Mn and Cr cases) the on-site correlations play a drastic role and taking them into account would push the Fe minority states higher in energy leading again to the opening of the gap in the minority density of states (DOS).³⁵ The same effect occurs also if we expand the lattice constant by 5 %, where the Fermi level is pushed deeper in the energy.¹⁹ Unfortunately the scheme used in Ref. 35 cannot be easily employed when disorder is present and it implicates the use of an ad-hoc parameter U (the so-called Hubbard parameter) which is not easily determined, and thus we do not take into account the on-site correlation effects in our study.

III. SUBSTITUTING Cr OR Fe FOR Mn IN Co_2MnZ ALLOYS

We will start our discussion from the two families of compounds containing both Co and Mn, where we sub-

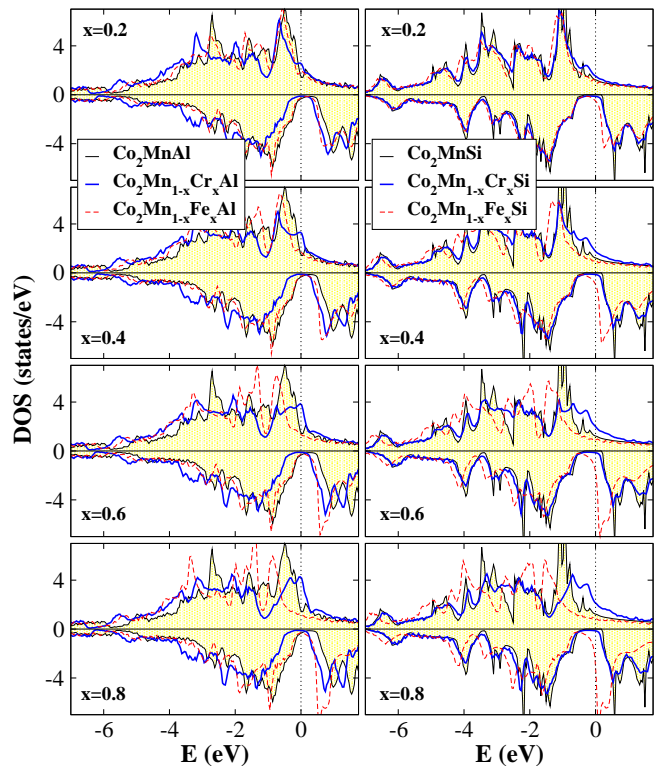


FIG. 3: (Color online) Total DOS in the case of the $\text{Co}_2[\text{Mn}_{1-x}(\text{Cr or Fe})_x]\text{Al}$ (left panel) and $\text{Co}_2[\text{Mn}_{1-x}(\text{Cr or Fe})_x]\text{Si}$ compounds (right panel) for four different values of the concentration x . The total DOS are compared with the ones of the perfect Co_2MnAl and Co_2MnSi compounds. Details as in Fig. 1.

stitute Fe and Cr for Mn. Substitution of Fe for Mn represents an increase of the total number of valence electrons, while the vice versa is true for the substitution of Cr for Mn. In Fig. 3 we have drawn the total DOS for the $\text{Co}_2[\text{Mn}_{1-x}(\text{Cr or Fe})_x]\text{Al}$ on the left column and for the Si-instead-of-Al compounds (right column) with respect to the perfect Co_2MnAl or Co_2MnSi alloys for different values of the concentration x .

As we stated in the previous section the Co_2CrAl and Co_2CrSi compounds are half-metals showing similar behavior to the Co_2MnAl and Co_2MnSi compounds. Thus also the intermediate quaternary compounds are half-metals. If the Z atom is Al or Ga, as we replace Cr for Mn, there is a leakage of charge from the majority states near the Fermi level towards the unoccupied majority states to account for the decrease in the average number of valence electrons. In the same time the change in the majority states influences also the exchange splitting and the minority bands move as in a rigid band lower in energy but the Fermi level remains within the gap (the minority blue line representing the quaternary compound moves lower in energy with the concentration with respect to the shaded region surrounded by the black line representing the ideal Co_2MnAl alloy). In the case of the Si, Ge and Sn (in the figure we show only the Si

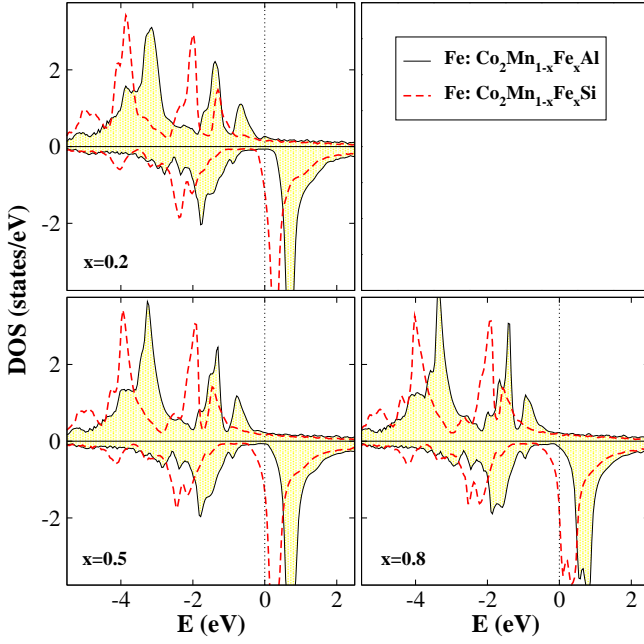


FIG. 4: (Color online) Fe-resolved DOS in the case of the $\text{Co}_2[\text{Mn}_{1-x}\text{Fe}_x]\text{Al}$ and $\text{Co}_2[\text{Mn}_{1-x}\text{Fe}_x]\text{Si}$ compounds for three different values of the concentration x . Details as in Fig. 1.

case) compounds, the alloys have one more valence electron and thus the exchange splitting between majority occupied Cr-Mn d-states and minority unoccupied Cr-Mn d-states is stronger and as we substitute Cr for Mn the minority states are almost identical to the one of the perfect Co_2MnSi alloy and only the majority states just below the Fermi level show a leakage towards unoccupied states to account for the decrease in the electron charge.

The reverse phenomena are present for the substitution of Fe for Mn. In the case of the $\text{Co}_2[\text{Mn}_{1-x}\text{Fe}_x]\text{Al}$ alloys the number of valence electrons is larger than for the $\text{Co}_2[\text{Mn}_{1-x}\text{Cr}_x]\text{Al}$ ones and they show behavior similar to the $\text{Co}_2[\text{Mn}_{1-x}\text{Cr}_x]\text{Si}$ family, showing small variations for the minority occupied states and the extra charge due to the increase in the Fe-concentration pushes some majority states below the Fermi level. The $\text{Co}_2[\text{Mn}_{1-x}\text{Fe}_x]\text{Al}$ compounds are half-metal for all the values of the concentration x although the gap is smaller than in the corresponding alloy with Cr-Mn mixing. The case of the compounds containing the heavier sp atoms like Si is more difficult since now already for the perfect Co_2MnSi there are 29 valence electrons. For the Co_2FeSi we have to fill 18 majority states (there are 12 minority occupied ones for the half-metallic full-Heusler alloys). This is difficult energetically since we have to occupy the high lying antibonding majority states and the system prefers to loose half-metallicity to gain energy. Kandpal and collaborators have argued that in this case the on-site correlation effects, which are not taken into account by conventional LSDA calculations, become important and they can reopen the gap and restore the half-metallicity.³⁵ To make this discussion more clear we have drawn in Fig.

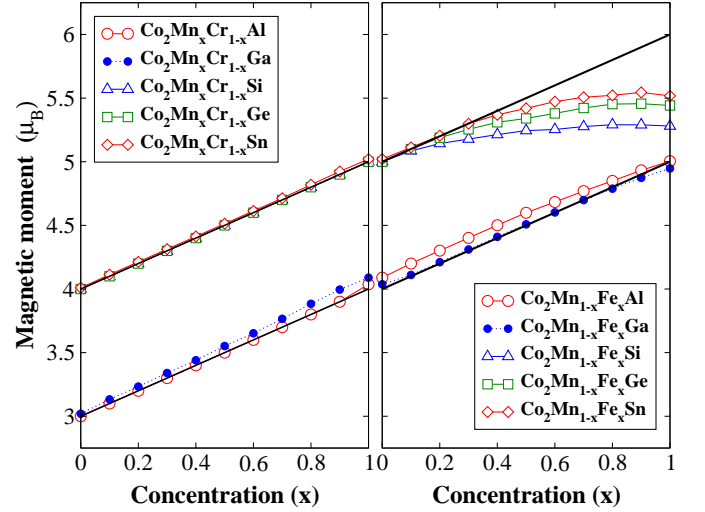


FIG. 5: (Color online) Total spin magnetic moment as a function of the concentration x for the studied $\text{Co}_2[\text{Mn}_{1-x}\text{Cr}_x]\text{Z}$ and $\text{Co}_2[\text{Mn}_{1-x}\text{Fe}_x]\text{Z}$ Heusler compounds. The solid black lines represent the Slater-Pauling behavior.

4 the Fe-resolved DOS for both $\text{Co}_2[\text{Mn}_{1-x}\text{Fe}_x]\text{Al}$ and $\text{Co}_2[\text{Mn}_{1-x}\text{Fe}_x]\text{Si}$ compounds for three different values of the concentration x . All graphs have been scaled to one atom. For the Al-based alloy Fe shows identical DOS irrespectively of its concentration in the quaternary alloy. On the other hand in the Si-based compound as the concentration of Fe in the alloy increases the extra charge occupies also minority states above the gap which now cross the Fermi level.

The above discussion on the total DOS and the question of the preservation of the half-metallicity in the quaternary compounds is reflected on the total spin moments and in Fig. 5 we have drawn the variation of the total spin moment as a function of the concentration x for all compounds under study in this section. The solid black lines represent the Slater-Pauling behavior obeyed by the perfect half-metallic ferromagnets. It is obvious that when the sp atom is either Al or its isoelectronic Ga the compounds show behavior very close to the SP one and thus although not perfect half-metals they present very high values of spin-polarization at the Fermi level. On the other hand compounds containing the heavier Si, Ge and Sn atoms are perfect half-metals when we mix Cr and Mn, but when we substitute Fe for Mn the half-metallicity is lost even for a concentration of Fe of 0.2. For concentration values between 0.4 and 1 the $\text{Co}_2[\text{Mn}_{1-x}\text{Fe}_x](\text{Si, Ge or Sn})$ total spin moments show a plateau being constant. We will discuss the smaller deviations for the Sn and Ge compounds with respect to the Si one in the next section since the same occurs also for the $\text{Co}_2[\text{Cr}_{1-x}\text{Fe}_x](\text{Si, Ge or Sn})$ alloys. Now the question arises what is the mechanism for this. In Table I we have gathered the atom-resolved spin moments for all compounds under study including also the $\text{Co}_2[\text{Cr}_{1-x}\text{Fe}_x]\text{Z}$ families. As we can see the Fe-resolved spin moment in

TABLE I: Total and atom-resolved spin magnetic moments for the case of the studied Al and Si compounds in μ_B . The total moment in the cell is the sum of the atomic ones multiplied by the concentration of this chemical element. Note that for Cr, Mn and Fe we have scaled the spin moments to one atom and that for Co we give the sum of the moments of both atoms.

x	$\text{Co}_2[\text{Cr}_{1-x}\text{Fe}_x]\text{Al}$					$\text{Co}_2[\text{Cr}_{1-x}\text{Fe}_x]\text{Si}$				
	Total	Co	Cr	Fe	sp	Total	Co	Cr	Fe	sp
0.00	3.00	1.46	1.63		-0.09	4.00	1.89	2.17		-0.09
0.20	3.40	1.72	1.49	2.89	-0.09	4.31	2.04	2.21	2.78	-0.08
0.40	3.80	1.87	1.47	2.86	-0.10	4.57	2.18	2.24	2.75	-0.08
0.60	4.19	2.02	1.48	2.83	-0.11	4.82	2.31	2.25	2.75	-0.07
0.80	4.58	2.15	1.50	2.80	-0.12	5.05	2.43	2.28	2.75	-0.07
1.00	4.95	2.27		2.79	-0.12	5.28	2.52		2.79	-0.06

x	$\text{Co}_2[\text{Mn}_{1-x}\text{Cr}_x]\text{Al}$					$\text{Co}_2[\text{Mn}_{1-x}\text{Cr}_x]\text{Si}$				
	Total	Co	Mn	Cr	sp	Total	Co	Mn	Cr	sp
0.00	4.04	1.36	2.82		-0.14	5.00	1.96	3.13		-0.09
0.20	3.80	1.54	2.74	0.91	-0.11	4.80	1.97	3.12	2.09	-0.08
0.40	3.60	1.55	2.77	1.20	-0.10	4.60	1.95	3.12	2.12	-0.08
0.60	3.40	1.54	2.79	1.37	-0.09	4.40	1.93	3.13	2.15	-0.07
0.80	3.20	1.53	2.83	1.48	-0.08	4.20	1.91	3.13	2.17	-0.07
1.00	3.00	1.46		1.63	-0.09	4.00	1.89		2.17	-0.06

x	$\text{Co}_2[\text{Mn}_{1-x}\text{Fe}_x]\text{Al}$					$\text{Co}_2[\text{Mn}_{1-x}\text{Fe}_x]\text{Si}$				
	Total	Co	Mn	Fe	sp	Total	Co	Mn	Fe	sp
0.00	4.04	1.36	2.82		-0.14	5.00	1.96	3.13		-0.09
0.20	4.21	1.58	2.76	2.79	-0.13	5.14	2.13	3.15	2.82	-0.08
0.40	4.41	1.76	2.78	2.79	-0.13	5.21	2.25	3.18	2.79	-0.07
0.60	4.60	1.94	2.82	2.79	-0.13	5.25	2.36	3.20	2.78	-0.05
0.80	4.79	2.12	2.86	2.79	-0.13	5.29	2.46	3.23	2.78	-0.04
1.00	4.95	2.27		2.79	-0.12	5.28	2.52		2.79	-0.03

the case of the $\text{Co}_2[\text{Mn}_{1-x}\text{Fe}_x]\text{Si}$ compounds is almost constant because the extra charge occupies equally majority and minority states and the number of uncompensated spin is almost constant. Since no increase in Fe spin-moment occurs and the Fe spin-moment is considerably smaller than the Mn one the total spin moment is not increased.

To complete this section we will briefly also discuss the atom-resolved spin moments of the different constituents (we will omit for the present any reference to the $\text{Co}_2[\text{Cr}_{1-x}\text{Fe}_x]\text{Z}$ alloys). Overall Mn, Fe and Cr atoms which play the role of the lower-valent transition-metal atom show stable constant spin moments irrespectively of the concentration. Cr in the case of Al and Ga based compounds has smaller moments than for the heavier Si, Ge or Sn-based compounds and this behavior is largely due to the relative position of the Fermi level with respect to the majority peak which it crosses. This behavior has been extensively discussed in Ref. 42. Mn has larger spin moment by about $0.3 \mu_B$ when the sp atom belong to the Si-column instead of the Al-one accounting for a small fraction of the extra electron. The fact that Mn shows a pretty standard behavior is also seen in Fig. 6 where we have drawn the Mn-resolved DOS for several cases. It is obvious that Mn DOS is similar for all cases under study with slight variations mainly due to the different

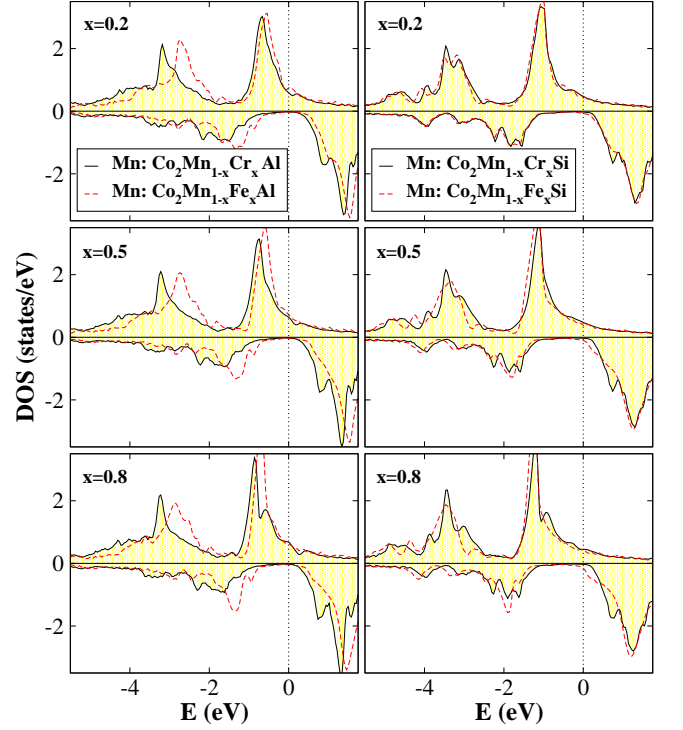


FIG. 6: (Color online) Mn-resolved DOS in the case of the $\text{Co}_2[\text{Mn}_{1-x}(\text{Cr or Fe})_x]\text{Al}$ (left panel) and $\text{Co}_2[\text{Mn}_{1-x}(\text{Cr or Fe})_x]\text{Si}$ (right panel) compounds for three different values of the concentration x . Details as in Fig. 1.

environment created by the Co atoms (each Mn atom has eight Co atoms as first neighbors) which carry also the information about the sp atoms and the Cr or Fe ones at the other sites. There are cases where the Mn-DOS is more spiky but this is entirely due to small shifts of the localized-in-energy e_g states with respect to the more delocalized t_{2g} ones.

Co atoms show a more interesting behavior. As we substitute Fe for Mn, Co atoms increase considerably their spin magnetic moment to account for the extra charge (the same occurs when we substitute Fe for Cr), while when we dope with Cr the spin-moment of the Co atoms is almost constant. Overall, as expected for the same type of compounds the Co has a larger moment when the sp atom is a Si-column one than a Al-column one due to the larger number of valence electrons. In Fig. 7 we have drawn the Co-projected DOS for all cases under study and for several values of the concentration x . Every Co atom is surrounded by four low-valent transition metal atoms (Cr, Mn or Fe) and four sp-atoms carrying the information for the different systems through the hybridization of the d-states of Co with the d-states of the other transition-metal atoms or the p-states of the sp-atom. As it was shown in Ref. 12 the minority states just around the gap (when there is a real gap) are exclusively located at Co sites. Thus when we mix Mn with Cr, where a real gap exists (DOS's with blue lines in the figure), the gap is fully determined by the Co minority

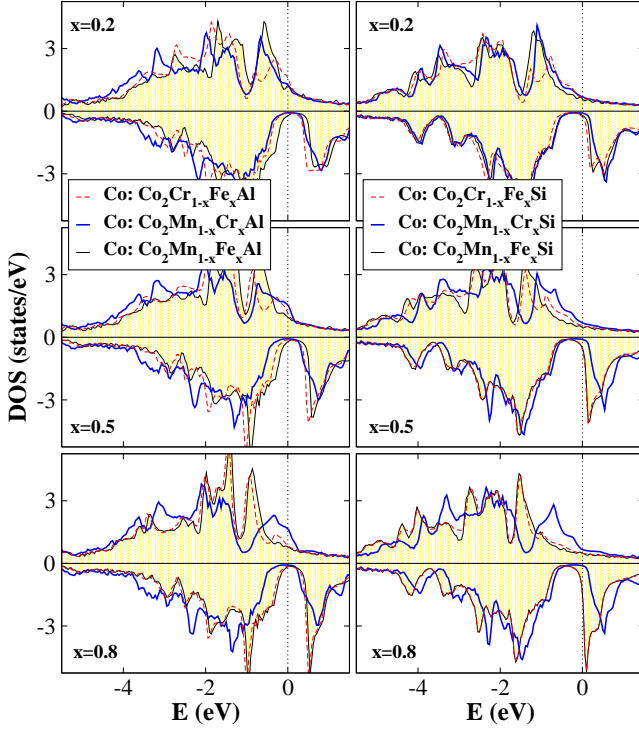


FIG. 7: (Color online) Co-resolved DOS in the case of the Al-based (left panel) and Si-based (right panel) compounds. Details as in Fig. 1.

states. For high concentration of Cr in $\text{Co}_2[\text{Mn}_{1-x}\text{Cr}_x]\text{Z}$, the Co atoms show a majority pick just below the Fermi level due to the large polarization induced by the Cr majority states at the Fermi level.¹⁹ In the case of compounds where Fe is present, both $\text{Co}_2[\text{Mn}_{1-x}\text{Fe}_x]\text{Z}$ and $\text{Co}_2[\text{Cr}_{1-x}\text{Fe}_x]\text{Z}$, Fe minority states are near the Fermi level (they even cross it) polarizing the Co d-states and the gap of the Co minority states becomes more narrow. This phenomenon is so intense, especially for large Fe concentrations, that the Co-DOS close to the Fermi level is identical for both families of compounds (red line for $\text{Co}_2[\text{Cr}_{1-x}\text{Fe}_x]\text{Z}$ and black shaded for $\text{Co}_2[\text{Mn}_{1-x}\text{Fe}_x]\text{Z}$). In general the variation of the spin moment of the Co atoms can be used to characterize the variation of the concentration in different perfectly ordered samples.

IV. THE CASE OF THE $\text{Co}_2\text{Cr}_{1-x}\text{Fe}_x\text{Z}$ FAMILY

In the last part of our study we investigated the properties of the $\text{Co}_2[\text{Cr}_{1-x}\text{Fe}_x]\text{Z}$ alloys with Z being Al, Ga, Si, Ge or Sn. As we have already mentioned above these compounds present properties very similar to the $\text{Co}_2[\text{Mn}_{1-x}\text{Fe}_x]\text{Z}$ families. Fe plays a central role even at relatively low concentrations affecting the half-metallicity. In Fig. 8 we have drawn the behavior of the total spin moments with the concentration x . The solid black lines represent the perfect SP behavior of the ideal half-metallic ferromagnets. For the case where Z is either

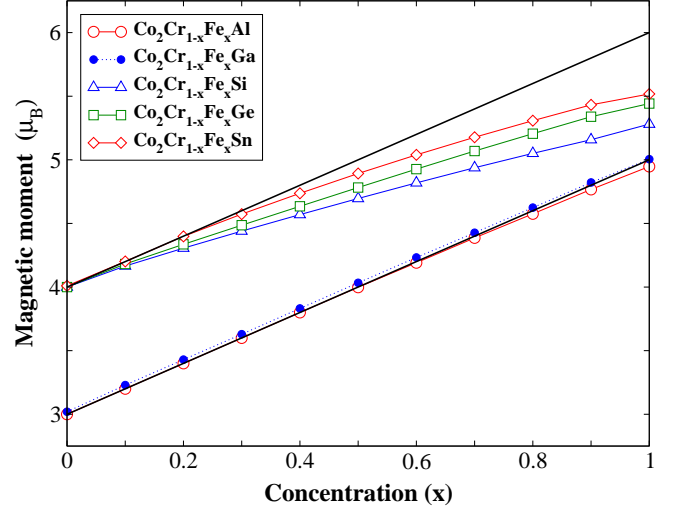


FIG. 8: (Color online) Total spin magnetic moment as a function of the concentration x for the studied $\text{Co}_2[\text{Cr}_{1-x}\text{Fe}_x]\text{Z}$ Heusler compounds. The solid black lines represent the Slater-Pauling behavior.

Al or Ga the total spin moment should vary between $3 \mu_B$ for the alloy containing only Cr ($x = 0$) and $5 \mu_B$ for the alloy containing exclusively Fe ($x = 1$). The Ga-based compound falls exactly on the solid black line and thus is half metallic for all concentrations. The Al compounds deviates slightly only for very high concentrations of Fe ($x = 0.9$ or 1). This is also observed in Table I where we present the atom-resolved and total spin moments. For $\text{Co}_2[\text{Cr}_{0.2}\text{Fe}_{0.8}]\text{Al}$ the total spin moment is 4.58 instead of the ideal 4.6 and for Co_2FeAl the total moment is 4.95 instead of the perfect value of 5. Of course a slight increase of the lattice constant will push the Fermi level deeper in energy and back in the gap and half-metallicity will be restored even in these cases.

On the other the total spin moments, in the case where Z is Si or its isoelectronic Ge and Sn, strongly deviate from the SP behavior showing similar behavior to the case of $\text{Co}_2[\text{Mn}_{1-x}\text{Fe}_x](\text{Si, Ge or Sn})$ compounds in Fig. 5. It is interesting that the Si compounds present in general lower values of total spin moment than the Ge and Sn ones in both cases (see Figs. 5 and 8). To elucidate this behavior we have included in Table II the total and atom resolved spin moment for $\text{Co}_2[(\text{Cr or Mn})_{1-x}\text{Fe}_x]\text{-Si}$ and -Sn compounds. The Co_2FeSi has a total spin moment of $5.28 \mu_B$ while Co_2FeSn shows a total spin moment of $5.52 \mu_B$. If we compare the trends between the Si and Sn compounds, we remark that the Mn and Fe spin moments are larger in the case of $\text{Z} = \text{Sn}$. Sn is a much heavier element than Si and the valence p electrons are more extended in space but this is over-compensated by the larger lattice constant. This larger lattice constant leads also to much smaller spin moments at the Sn site since a larger number of majority states is occupied than for Si. Since the lattice constant is larger, Mn and Fe atoms have more space around them and thus

TABLE II: Total and atom-resolved spin magnetic moments for the case of the studied $\text{Co}_2[\text{Cr}_{1-x}\text{Fe}_x](\text{Si or Sn})$ in μ_B .

x	$\text{Co}_2[\text{Cr}_{1-x}\text{Fe}_x]\text{Si}$					$\text{Co}_2[\text{Cr}_{1-x}\text{Fe}_x]\text{Sn}$				
	Total	Co	Cr	Fe	sp	Total	Co	Cr	Fe	sp
0.00	4.00	1.89	2.17		-0.09	4.00	1.66	2.41		-0.06
0.20	4.31	2.04	2.21	2.78	-0.08	4.40	1.89	2.49	2.89	-0.06
0.40	4.57	2.18	2.24	2.75	-0.08	4.74	2.10	2.54	2.89	-0.05
0.60	4.82	2.31	2.25	2.75	-0.07	5.04	2.30	2.60	2.90	-0.04
0.80	5.05	2.43	2.28	2.75	-0.07	5.31	2.47	2.65	2.92	-0.02
1.00	5.28	2.52		2.79	-0.06	5.52	2.61		2.92	-0.01

x	$\text{Co}_2[\text{Mn}_{1-x}\text{Fe}_x]\text{Si}$					$\text{Co}_2[\text{Mn}_{1-x}\text{Fe}_x]\text{Sn}$				
	Total	Co	Mn	Fe	sp	Total	Co	Mn	Fe	sp
0.00	5.00	1.96	3.13		-0.09	5.02	1.78	3.32	2.91	-0.08
0.20	5.14	2.13	3.15	2.82	-0.08	5.20	1.98	3.38	2.93	-0.07
0.40	5.21	2.25	3.18	2.79	-0.07	5.37	2.19	3.44	2.93	-0.05
0.60	5.25	2.36	3.20	2.78	-0.05	5.47	2.36	3.45	2.93	-0.04
0.80	5.29	2.46	3.23	2.78	-0.04	5.52	2.49	3.53	2.94	-0.03
1.00	5.28	2.52		2.79	-0.03	5.52	2.61		2.92	-0.01

a larger Wigner-Seitz sphere and their behavior becomes more atomic-like leading to an increase of their atomic spin moments and thus to larger total spin moments. The same phenomenon is also true for the compounds containing Ge.

We will finish our investigation by examining the behavior of the atoms in the different compounds. In Table I we have included the atomic spin moments for the $\text{Co}_2[\text{Cr}_{1-x}\text{Fe}_x]\text{Al}$ (upper left panel) and $\text{Co}_2[\text{Cr}_{1-x}\text{Fe}_x]\text{Si}$ (upper right panel) and in Fig. 9 we have drawn the Cr-resolved DOS in the left panel and the Fe-resolved one in the right panel for both Al- (solid black lines with shaded area) and Si-based (red dashed lines) compounds for three different values of the concentration $x=0.2, 0.5$ and 0.8 . As we mentioned in the previous section, Co atoms increase considerably their spin moments to account for the extra charge as we dope with Fe. On the other hand Cr and Fe atoms have a pretty constant spin moment through out all the concentrations range. Cr has a spin moment of around $1.5 \mu_B$ in the Al-based compound and around $2.2 \mu_B$ in the heavier Si-based compound. Fe on the other hand in the Si compound cannot increase any more its spin moment with respect to the Al compound and has a slight portion of its minority states above the gap occupied and thus its spin moment is slightly smaller for the heavier Si-compound than for the Al-one and this is the main reason for the failure of the compounds containing Fe and Si (or Ge or Sn) to retain the half-metallicity.

The discussion in the previous paragraphs in this Section is directly reflected on the atom-resolved DOS in Fig. 9. Cr in $\text{Co}_2[\text{Cr}_{1-x}\text{Fe}_x]\text{Al}$ has an expected shape of DOS with the Fermi level being pinned exactly at the maximum of the pick of the majority states contrary to the case of the $\text{Co}_2[\text{Mn}_{1-x}\text{Cr}_x]\text{Al}$ compounds where it was below this maximum and was shifted towards it as the Cr concentration increased (see Ref. 42). Substituting Si for Al provides extra electrons and the majority

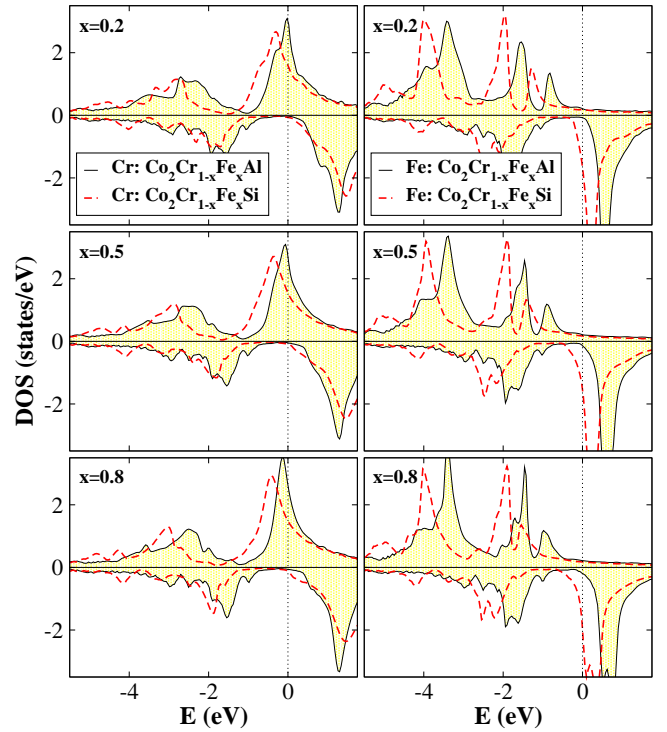


FIG. 9: (Color online) Cr- (left panel) and Fe-resolved (right panel) DOS in the case of the $\text{Co}_2[\text{Cr}_{1-x}\text{Fe}_x]\text{Al}$ and $\text{Co}_2[\text{Cr}_{1-x}\text{Fe}_x]\text{Si}$ compounds for three different values of the concentration x . Details as in Fig. 1.

states are pushed deeper in energy being accompanied by a similar movement of the minority states as in a rigid band model. But this shift is not strong enough to lead to the loss of half-metallicity and the Fermi level is located at the higher-energy-edge of the gap. These features for the Si compound are similar to the ones of the perfect Co_2CrSi studied recently by Chen et al.¹⁹ On the other hand Fe majority states are deep in energy (Fe has two more electrons than Cr) and for the Al-compound the Fermi level falls at the higher-energy-edge of the minority gap which corresponds to a region of very low majority DOS. When we pass from Al to Si which has one valence electron more, the unoccupied states just above the Fermi level cannot absorb the extra charge and it would cost a lot in energy to occupy states far above the Fermi level and thus the system prefers to occupy also minority states and to loose its half-metallicity.

V. CONCLUSIONS

We have complemented our study on the doping and disorder in Co_2MnZ compounds presented in Refs. 40 and 42 studying the quaternary $\text{Co}_2[\text{Y}_{1-x}\text{Y}_x^*]\text{Z}$ compounds with the lower-valent transition metals Y, Y* being Cr, Mn or Fe and the sp atom Z being one of Al, Ga, Si, Ge, Sn. Thus this study gave us a global overview of the magnetic and electronic properties of these com-

pounds. The most important desirable feature of these compounds is half-metallicity combined with high values of the majority density of states at the Fermi level. The latter feature would enable the good operation of the devices even when the half-metallic character is lost due to defects, creation of interfaces or temperature-driven phenomena. Our study shows that the high values of majority density of states at the Fermi level are ensured by the presence of Cr at high concentrations while the only factor susceptible of destroying the half-metallicity is the simultaneous presence of Fe and Si (or Ge or Sn) in the compound. Moreover the presence of Cr or Mn and the exclusion of Fe is responsible for larger minority band-gaps and thus for more stable half-metallicity with respect to the phenomena which can induce states within the gap.

To summarize, our results suggest that for realistic ap-

plications the most appropriate compounds are the ones belonging to the families $\text{Co}_2[\text{Mn}_{1-x}\text{Cr}_x]\text{Z}$ with $x > 0.5$ irrespectively of the nature of *sp* atoms since they combine high values of majority DOS at the Fermi level, and half-metallicity with large band-gaps. On the other hand the presence of Fe lowers considerably the majority density of states at the Fermi level and when combined with an element belonging to the Si-column, it even can destroy half-metallicity.

Acknowledgements

Authors acknowledge the computer support of the “Leibniz Institute for Solid State and Materials Research Dresden”.

-
- * Electronic address: kozdogan@gyte.edu.tr
† Electronic address: galanakis@upatras.gr
‡ Electronic address: e.sasioglu@fz-juelich.de
- ¹ I. Žutić, J. Fabian, and S. Das Sarma, *Rev. Mod. Phys.* **76**, 323 (2004).
 - ² Half-metallic alloys: fundamentals and applications, Eds.: I. Galanakis and P. H. Dederichs, *Lecture notes in Physics* vol. 676 (Berlin Heidelberg: Springer 2005).
 - ³ I. Galanakis, Ph. Mavropoulos, and P. H. Dederichs, *J. Phys. D: Appl. Phys.* **39**, 765 (2006); I. Galanakis and Ph. Mavropoulos, *J. Phys.: Condens. Matter* in press (cond-mat/0610827)
 - ⁴ A. Bergmann, J. Grabis, B. P. Toperverg, V. Leiner, M. Wolff, H. Zabel, and K. Westerholt, *Phys. Rev. B* **72**, 214403 (2005); J. Grabis, A. Bergmann, A. Nefedov, K. Westerholt, and H. Zabel, *Phys. Rev. B* **72**, 024437 (2005); *idem*, *Phys. Rev. B* **72**, 024438 (2005).
 - ⁵ S. Kämmerer, A. Thomas, A. Hütten, and G. Reiss, *Appl. Phys. Lett.* **85**, 79 (2004); J. Schmalhorst, S. Kämmerer, M. Sacher, G. Reiss, A. Hütten, and A. Scholl, *Phys. Rev. B* **70**, 024426 (2004).
 - ⁶ Y. Sakuraba, M. Hattori, M. Oogane, Y. Ando, H. Kato, A. Sakuma, T. Miyazaki, and H. Kubota, *Appl. Phys. Lett.* **88**, 192508 (2006); Y. Sakuraba, J. Nakata, M. Oogane, Y. Ando, H. Kato, A. Sakuma, T. Miyazaki, and H. Kubota, *Appl. Phys. Lett.* **88**, 022503 (2006); Y. Sakuraba, T. Miyakoshi, M. Oogane, Y. Ando, A. Sakuma, T. Miyazaki, and H. Kubota, *Appl. Phys. Lett.* **89**, 052508 (2006); Y. Sakuraba, J. Nakata, M. Oogane, H. Kubota, Y. Ando, A. Sakuma, and T. Miyazaki, *Jpn. J. Appl. Phys.* **44**, L1100 (2005); Y. Sakuraba, J. Nakata, M. Oogane, H. Kubota, Y. Ando, A. Sakuma, and T. Miyazaki, *Jpn. J. Appl. Phys.* **44**, 6535 (2005).
 - ⁷ X. Y. Dong, C. Adelman, J. Q. Xie, C. J. Palmström, X. Lou, J. Strand, P. A. Crowell, J.-P. Barnes, and A. K. Petford-Long, *Appl. Phys. Lett.* **86**, 102107 (2005).
 - ⁸ R. A. de Groot, F. M. Mueller, P. G. van Engen, and K. H. J. Buschow, *Phys. Rev. Lett.* **50**, 2024 (1983).
 - ⁹ P. J. Webster, *J. Phys. Chem. Solids* **32**, 1221 (1971).
 - ¹⁰ S. Ishida, S. Fujii, S. Kashiwagi, and S. Asano, *J. Phys. Soc. Jpn.* **64**, 2152 (1995); S. Fujii, S. Sugimura, S. Ishida, and S. Asano, *J. Phys.: Condens. Matter* **2**, 8583 (1990).
 - ¹¹ S. Picozzi, A. Continenza, and A. J. Freeman, *Phys. Rev. B* **66**, 094421 (2002).
 - ¹² I. Galanakis, P. H. Dederichs, and N. Papanikolaou, *Phys. Rev. B* **66**, 174429 (2002).
 - ¹³ M. P. Raphael, B. Ravel, M. A. Willard, S. F. Cheng, B. N. Das, R. M. Stroud, K. M. Bussmann, J. H. Claassen, and V. G. Harris, *Appl. Phys. Lett.* **79**, 4396 (2001); B. Ravel, M. P. Raphael, V. G. Harris, and Q. Huang, *Phys. Rev. B* **65**, 184431 (2002); F. Y. Yang, C. H. Shang, C. L. Chien, T. Ambrose, J. J. Krebs, G. A. Prinz, V. I. Nikitenko, V. S. Gornakov, A. J. Shapiro, and R. D. Shull, *Phys. Rev. B* **65**, 174410 (2002); T. Ambrose, J. J. Krebs, and G. A. Prinz, *Appl. Phys. Lett.* **76**, 3280 (2000).
 - ¹⁴ W. H. Wang, M. Przybylski, W. Kuch, L. I. Chelaru, J. Wang, Y. F. Lu, J. Barthel, H. L. Meyerheim, and J. Kirschner, *Phys. Rev. B* **71**, 144416 (2005); S. Wurmehl, G. H. Fecher, H. C. Kandpal, V. Ksenofontov, C. Felser, H.-J. Lin, and J. Morais, *Phys. Rev. B* **72**, 184434 (2005); R. Y. Umetsu, K. Kobayashi, R. Kainuma, A. Fujita, K. Fukamichi, K. Ishida, and A. Sakuma, *Appl. Phys. Lett.* **85**, 2011 (2004); L. Ritchie, G. Xiao, Y. Ji, T. Y. Chen, C. L. Chien, M. Zhang, J. Chen, Z. Liu, G. Wu, and X. X. Zhang, *Phys. Rev. B* **68**, 104430 (2003).
 - ¹⁵ M. P. Raphael, B. Ravel, Q. Huang, M. A. Willard, S. F. Cheng, B. N. Das, R. M. Stroud, K. M. Bussmann, J. H. Claassen, and V. G. Harris, *Phys. Rev.* **66**, 104429 (2002).
 - ¹⁶ K. Yakushiji, K. Saito, S. Mitani, K. Takanashi, Y. K. Takahashi, and K. Hono, *Appl. Phys. Lett.* **88**, 222504 (2006); M. Hashimoto, J. Herfort, H.-P. Schönherr, and K. H. Ploog, *Appl. Phys. Lett.* **87**, 102506 (2005).
 - ¹⁷ N.-N. Liu, A. Thomas, G. Reiss, and A. Hütten, *Appl. Phys. Lett.* **89**, 162506 (2006); Z. Gercsi, A. Rajanikanth, Y. K. Takahashi, K. Hono, M. Kikuchi, N. Tezuka, and K. Inomata, *Appl. Phys. Lett.* **89**, 082512 (2006).
 - ¹⁸ N. Tezuka, N. Ikeda, A. Miyazaki, S. Sugimoto, M. Kikuchi, and K. Inomata, *Appl. Phys. Lett.* **89**, 112514 (2006); S. Okamura, A. Miyazaki, S. Sugimoto, N. Tezuka, and K. Inomata, *Appl. Phys. Lett.* **86**, 232503 (2005).
 - ¹⁹ X.-Q. Chen, R. Podloucky, and P. Rogl, *J. Appl. Phys.* **100**, 113901 (2006).

- ²⁰ I. Galanakis, J. Phys.: Condens. Matter **14**, 6329 (2002).
- ²¹ K. Nagao, Y. Miura, and M. Shirai, Phys. Rev. B **73**, 104447 (2006); I. Galanakis, J. Phys.: Condens. Matter, **16**, 8007 (2004).
- ²² S. J. Hashemifar, P. Kratzer, and M. Scheffler, Phys. Rev. Lett. **94**, 096402 (2005).
- ²³ L. Chioncel, E. Arrigoni, M. I. Katsnelson, and A. I. Lichtenstein, Phys. Rev. Lett. **96**, 137203 (2006); L. Chioncel, M. I. Katsnelson, R. A. de Groot, and A. I. Lichtenstein, Phys. Rev. B **68**, 144425 (2003).
- ²⁴ M. Ležaić, Ph. Mavropoulos, J. Enkovaara, G. Bihlmayer, and S. Blügel, Phys. Rev. Lett. **97**, 026404 (2006).
- ²⁵ R. Skomski and P. A. Dowben, Europhys. Lett. **58**, 544 (2002).
- ²⁶ S. Picozzi, A. Continenza, and A. J. Freeman, Phys. Rev. B **69**, 094423 (2004).
- ²⁷ I. Galanakis, Phys. Rev. B **71**, 012413 (2005).
- ²⁸ T. Block, M. J. Carey, B. A. Gurney, and O. Jepsen, Phys. Rev. B **70**, 205114 (2004).
- ²⁹ E. Şaşıoğlu, L. M. Sandratskii, P. Bruno, and I. Galanakis, Phys. Rev. B **72**, 184415 (2005).
- ³⁰ Y. Kurtulus, R. Dronskowski, G. D. Samolyuk, and V. P. Antropov, Phys. Rev. B **71**, 014425 (2005).
- ³¹ I. Galanakis, J. Phys.: Condens. Matter **16**, 3089 (2004).
- ³² V. N. Antonov, H. A. Dürr, Yu. Kucherenko, L. V. Bekenov, and A. N. Yaresko, Phys. Rev. B **72**, 054441 (2005).
- ³³ Y. Miura, K. Nagao, and M. Shirai, Phys. Rev. B **69**, 144413 (2004).
- ³⁴ B. Balke, G. H. Fecher, H. C. Kandpal, C. Felser, K. Kobayashi, E. Ikenaga, J.-J. Kim, and S. Ueda, Phys. Rev. B **74**, 104405 (2006).
- ³⁵ H. M. Kandpal, G. H. Fecher, C. Felser, and G. Schönhausen, Phys. Rev. B **73**, 094422 (2006).
- ³⁶ S. Wurmehl, G. H. Fecher, H. C. Kandpal, V. Ksenofontov, C. Felser, and H.-J. Lin, Appl. Phys. Lett. **88**, 032503 (2006).
- ³⁷ A. D. Rata, H. Braak, D. E. Bürgler, S. Cramm, and C. M. Schneider, Eur. Phys. J. B **52**, 445 (2006); M. Kallmayer H. Schneider, G. Jakob, H. J. Elmers, K. Kroth, H. C. Kandpal, U. Stumm, and S. Cramm, Appl. Phys. Lett. **88**, 072506 (2006); S. V. Karthik, A. Rajanikanth, Y. K. Takahashi, T. Okhubo, and K. Hono, Appl. Phys. Lett. **89**, 052505 (2006); G. H. Fecher, H. C. Kandpal, S. Wurmehl, J. Morais, H.-J. Lin, H.-J. Elmers, G. Schönhausen, and C. Felser, J. Phys.: Condens. Matter **17**, 7237-7252 (2005); R. Y. Umetsu, K. Kobayashi, A. Fujita, K. Oikawa, R. Kainuma, K. Ishida, N. Endo, K. Fukamichi, and A. Sakuma, Phys. Rev. B **72**, 214412 (2005); K. Kobayashi, R. Y. Umetsu, R. Kainuma, K. Ishida, T. Oyamada, A. Fujita, and K. Fukamichi, Appl. Phys. Lett. **85**, 4684 (2004); H. J. Elmers, G. H. Fecher, D. Valdaitsev, S. A. Nepijko, A. Gloskovskii, G. Jakob, G. Schönhausen, S. Wurmehl, T. Block, C. Felser, P.-C. Hsu, W.-L. Tsai, and S. Cramm, Phys. Rev. B **67**, 104412 (2003); J. M. De Teresa, D. Serate, R. Cordoba, and S.M. Yusuf, J. Alloys Comp., in press.
- ³⁸ T. Marukame, T. Ishikawa, K.-I. Matsuda, T. Uemura, and M. Yamamoto, Appl. Phys. Lett. **88**, 262503 (2006); T. Marukame, T. Kasahara, K. Matsuda, T. Uemura T and M. Yamamoto, Jpn. J. Appl. Phys. **44**, L521 (2005).
- ³⁹ R. Kelekar and B. M. Klemens, Appl. Phys. Lett. **86**, 232501 (2005).
- ⁴⁰ I. Galanakis, K. Özdoğan, B. Aktaş, and E. Şaşıoğlu, Appl. Phys. Lett. **89**, 042502 (2006).
- ⁴¹ K. Koepernik and H. Eschrig, Phys. Rev. B **59**, 3174 (1999); K. Koepernik, B. Velicky, R. Hayn, and H. Eschrig, Phys. Rev. B **58**, 6944 (1998).
- ⁴² K. Özdoğan, E. Şaşıoğlu, B. Aktaş, and I. Galanakis, Phys. Rev. B **74**, (2006).
- ⁴³ P. J. Webster and K. R. A. Ziebeck, in *Alloys and Compounds of d-Elements with Main Group Elements. Part 2.*, edited by H. R. J. Wijn, Landolt-Boörnstein, New Series, Group III, Vol. 19,Pt.c (Springer-Verlag, Berlin 1988), pp. 75-184.
- ⁴⁴ K. R. A. Ziebeck and K.-U. Neumann, in *Magnetic Properties of Metals*, edited by H. R. J. Wijn, Landolt-Börnstein, New Series, Group III, Vol. 32/c (Springer Berlin 2001), pp. 64-414.